PAPER

Check for updates

Simultaneous electrochemical detection of Cd²⁺ and Pb²⁺ using a green silver nanoparticles/polyaniline-modified carbon paste electrode

Djihane Slimane Ben Ali, [ID] [ab] Ferial Krid,[ac] Ahlem Sarra Saadi,[ab] Mouna Nacef, [ID] *[d] Habiba Tabet[c] and Mohamed Lyamine Chelaghmia [ID] [d]

In this study, a novel electrochemical sensor based on a carbon paste electrode (CPE) modified with polyaniline (PANI) and green-synthesized silver nanoparticles (AgNPs) was developed for the simultaneous detection of cadmium (Cd^{2+}) and lead (Pb^{2+}) ions in aqueous solutions. The AgNPs were synthesized using a green route employing plant extract as a reducing and capping agent, ensuring environmental sustainability. The modified electrode (AgNPs-PANI-CPE) was characterized by UV-Vis spectroscopy, field-emission gun scanning electron microscopy (FEG-SEM), and simultaneous thermal analysis (TGA/DSC). The electrochemical behavior of Cd^{2+} and Pb^{2+} was investigated using square wave voltammetry (SWV) and CV. The sensor exhibited distinct and well-separated anodic peaks for Cd^{2+} and Pb^{2+}, with excellent sensitivity, wide linear response ranges, and low detection limits (0.09 and 0.05 µg L^{-1}, respectively). Interference studies demonstrated good selectivity towards the target ions, and successful application to real water samples confirmed its analytical performance. This work highlights the potential of eco-friendly nanocomposite-modified electrodes in environmental monitoring of toxic heavy metals.

1. Introduction

Heavy metal contamination in aquatic environments has become a major global concern due to its detrimental impact on ecosystems and human health. Among these metals, cadmium (Cd^{2+}) and lead (Pb^{2+}) are particularly toxic even at trace levels. These ions can accumulate in biological tissues, causing neurological, renal, and developmental disorders.[1,2] The World Health Organization has set very low permissible limits for Cd^{2+} (0.003 mg L^{-1}) and Pb^{2+} (0.1 mg L^{-1}) in drinking water due to their high toxicity.[3] Electochemical techniques have emerged as powerful tools for the detection of trace metals due to their high sensitivity, simplicity, low cost, and potential for miniaturization.[4] Among them, cyclic voltammetry (CV) and square wave voltammetry (SWV) are widely employed for qualitative and quantitative analysis of metal ions.[5,6] However, the selectivity and sensitivity of these methods largely depend on the nature and properties of the working electrode.

Carbon paste electrodes (CPE) are particularly attractive in electroanalysis due to their renewability, low background current, and ease of surface modification.[7] The incorporation of conductive polymers such as polyaniline (PANI) can significantly enhance the electrochemical properties of CPE. PANI is known for its good environmental stability, high electrical conductivity, and strong chelating ability towards metal ions, making it a suitable matrix for preconcentration and detection of heavy metals.[8–13]

In recent years, green-synthesized silver nanoparticles (AgNPs) have garnered significant attention for their excellent catalytic and electron transfer properties.[14–17] Unlike conventional chemical synthesis methods, green synthesis utilizes plant extracts or biological agents, offering an environmentally friendly, cost-effective, and scalable approach.[18] AgNPs possess a high surface area and unique surface plasmon resonance, which not only improve the electron transfer rate but also facilitate metal ion adsorption through surface interactions.[19]

Combining PANI with green-synthesized AgNPs to modify CPE provides a synergistic effect, resulting in enhanced electrochemical performance for the detection of metal ions. This composite material can offer improved sensitivity, selectivity, and lower detection limits for the simultaneous detection of Cd^{2+} and Pb^{2+}. Previous studies have shown that nanocomposite-modified electrodes can successfully differentiate the redox signals of multiple heavy metal ions.[20,21]

ªDepartment of Process Engineering, Faculty of Technology, Université 20 Août 1955, El Hadaik Road, Skikda 21000, Algeria. E-mail: dj.slimanebenali@univ-skikda.dz; djihanosse9@gmail.com

ᵇLRPCSI-Laboratoire de Recherche sur la Physico-Chimie des Surfaces et Interfaces, Université 20 Août 1955, Skikda 21000, Algeria

ᶜChemical and Environmental Engineering Research Laboratory, LGCE, Algeria

ᵈLAIGM, Université 8 Mai 1945 Guelma, BP 401, Guelma 24000, Algeria

In this research, we developed a new electrochemical sensor for simultaneous determination of Cd^{2+}, Pb^{2+} using square wave voltammetry (SWV) and cyclic voltammetry (CV) with high sensitivity and low detection limit.

For the first time, we report the use of a new carbon paste electrode based on low-cost pencil graphite powder modified with PANI and green synthesized silver nanoparticles using olive leaves extract.

2. Experimental

2.1. Chemicals and reagents

All reagents were of analytical grade and used without any further purification. Lead nitrate ($Pb(NO_3)_2$, ≥99.0%) and cadmium nitrate tetrahydrate ($Cd(NO_3)_2 \cdot 4H_2O$, ≥99.0%) were purchased from Sigma-Aldrich. Silver nitrate ($AgNO_3$, 99.0%), aniline monomer (≥99.5%), concentrated sulfuric acid (H_2SO_4, 95–98%), and paraffin oil (≥99.0%) were obtained from Merck. Fresh olive leaves were collected locally, washed thoroughly with distilled water, and dried under ambient conditions. Rotring® pencil graphite B grade was bought in a local library.[8]

2.2. Apparatus and measurements

The fabricated electrode was characterized through a combination of techniques. The surface morphology of the electrode materials was examined using field-emission scanning electron microscopy (FEG-SEM, Quattro S), along with elemental composition analysis. Thermal stability was evaluated using a simultaneous thermal analyzer (TGA/DSC: TGA/DTG 3 + 1600 °C, Mettler Toledo). Electrochemical measurements were conducted using either a potentiostat/galvanostat 273A or a VersaSTAT 3 potentiostat/galvanostat (Princeton Applied Research, AMETEK, USA). The latter was specifically employed for electrochemical impedance spectroscopy (EIS). All measurements were carried out using a conventional three-electrode system consisting of a platinum wire as the counter electrode, an Ag/AgCl (saturated KCl) reference electrode, and the modified carbon paste electrodes as the working electrodes. All potentials are reported with respect to the Ag/AgCl (saturated KCl) reference electrode.

2.3. Green synthesis of silver nanoparticles (AgNPs)

Fresh olive leaves (20 g) were boiled in 100 mL of distilled water at 80 °C for 30 minutes. After cooling, the extract was filtered and stored at 4 °C. For the synthesis of AgNPs, 10 mL of the olive leaf extract was added dropwise to 90 mL of 1 mM $AgNO_3$ solution under continuous stirring at room temperature. The reaction was monitored by UV-Vis spectroscopy. A color change to dark brown indicated the formation of AgNPs. The solution was centrifuged at 10 000 rpm for 15 min, and the nanoparticles were washed and dried for further use to obtain a metallic powder appearance.[22,23]

2.4. Electropolymerization of polyaniline (PANI)

Polyaniline was electrochemically polymerized onto a graphite substrate in a 0.1 M aniline solution containing 1 M H_2SO_4 by cyclic voltammetry (CV) in the potential range of −0.2 V to +1.0 V vs. Ag/AgCl at a scan rate of 50 mV s^{-1} for 10 cycles. The polymerized film was washed with distilled water to remove excess monomer and dried at room temperature.[24]

2.5. Preparation of the modified carbon paste electrode (AgNPs-PANI-CPE)

Carbon paste was prepared by thoroughly mixing 90 g finely grounded pencil graphite powder with ten drops of paraffin oil in a mortar until a homogenous or at least 20 min till a smoothly wetted and suitably firm paste texture was achieved. To fabricate the modified electrode: a portion of the paste was mixed with a known amount of dried AgNPs for at least 20 min till a smoothly wetted and suitably firm paste texture was achieved. The paste was filled and packed in a glass cylinder with 9 mm of diameter and 60 mm of length. A copper wire was sealed to a plunger that was in close contact with the paste and extended to the outside of the cylinder to ensure electrical contact.

A polyaniline film was deposited on the surface by drop-coating a small amount of PANI dispersion and allowing it to dry.[8]

2.6. Electrochemical measurements

Supporting electrolyte was typically 0.1 M acetate buffer (pH 4.5). The accumulation potential and time, scan parameters, and peak separation were optimized for simultaneous detection of Cd(II) and Pb(II), and the optimum amplitude used for SWV was 25 mV.

2.7. Real sample preparation

Tap water and synthetic seawater samples were filtered and spiked with known concentrations of Cd^{2+} and Pb^{2+} for recovery studies. The electrochemical response was measured under optimized conditions.

2.8. Statistical analysis and calibration

All experiments, including electrochemical (SWV, CV, EIS) and spectroscopic (UV-Vis, TGA) measurements, were performed in triplicate ($n = 3$) to ensure reproducibility and reliability. Results are reported as mean ± standard deviation (SD).

The limit of detection (LOD) and quantitation limit (QL) were estimated based on the standard deviation and slope of the calibration curve, as described in the ICH guideline,[25] respectively.

$$DL = 3.3\ SD/S1$$

$$QL = 10\ SD/S2$$

Sensitivity was derived from the slope of the linear regression equation obtained from calibration plots.

All calibration curves include error bars representing ± standard deviation from three independent measurements. The graphs shown in the manuscript are representative of these repeated measurements.

3. Results and discussion

3.1. Material characterization

Fig. 1 illustrates the morphological characteristics of the prepared electrode. As shown in Fig. 1A, the synthesized polyaniline (PANI) exhibits a sponge-like morphology with large porous structures and small rod-shaped particles with an average diameter of approximately 41 nm, in agreement with previously reported studies.[26,27] In contrast, Fig. 1B shows that the unmodified carbon paste electrode, prepared using paraffin oil, presents a relatively smooth and homogeneous surface.[8]

Fig. 2 representative thermograms obtained from triplicate measurements.

The thermogravimetric analysis of polyaniline, Fig. 2 showed 3 main thermal degradation stages. The first thermal degradation was observed at 100–150 °C, corresponding to a derivative thermogravimetry (DTG) endothermic peak centered at 105 related to the evaporation of physically adsorbed water. This is a common feature for hygroscopic materials like PANI. A more gradual and steady weight loss is seen in the range [200; 400 °C], which is generally attributed to the loss of dopant molecules and low molecular weight oligomers present in the PANI structure. A sharp and significant weight loss (endothermic peak, Fig. 2 curve B) at ~600 °C, indicating the most intense decomposition in relation with to the thermal degradation of the polymer backbone of PANI. Beyond 800 °C, the curve flattens, indicating that most of the decomposable organic material has been lost, and only carbonaceous residues remained.[28]

The FT-IR spectrum of the olive leaf extract reveals several characteristic absorption bands in Fig. 3a indicating the presence of various bioactive functional groups involved in the green synthesis and stabilization of silver nanoparticles.
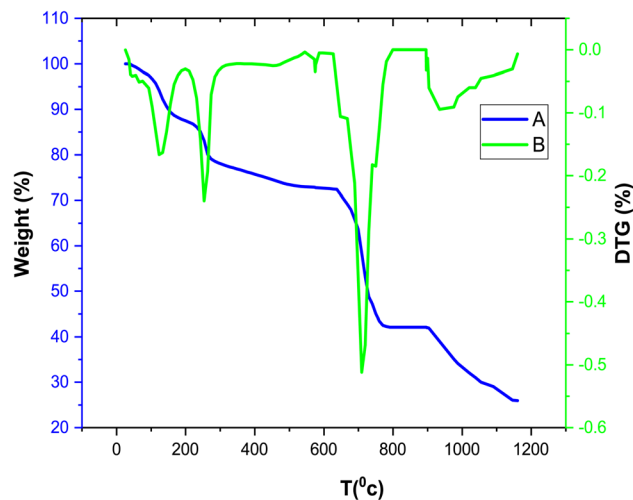

Fig. 2 The thermogravimetric analysis (TGA) and derivative thermogravimetric (DTG) data of polyaniline (PANI), with curve A (in blue) showing the TGA curve and curve B (in green) the DTG curve.

The broad and intense band centered at 3303 cm^{-1} is attributed to the O–H stretching vibrations of hydroxyl groups, commonly present in polyphenols and flavonoids.

Peaks at 2926 cm^{-1} and 2854 cm^{-1} correspond to C–H stretching vibrations of aliphatic $–CH_2^-$ groups, suggesting the presence of aliphatic chains in the extract.

A weak band near 2369 cm^{-1} is possibly due to O=C=O stretching of atmospheric CO_2 or residual carbonyl-containing compounds.

The absorption band around 1633 cm^{-1} is associated with C=O stretching of conjugated carbonyls or C=C stretching of aromatic rings.

The peak at 1329 cm^{-1} corresponds to C–N stretching vibrations from aromatic amines.
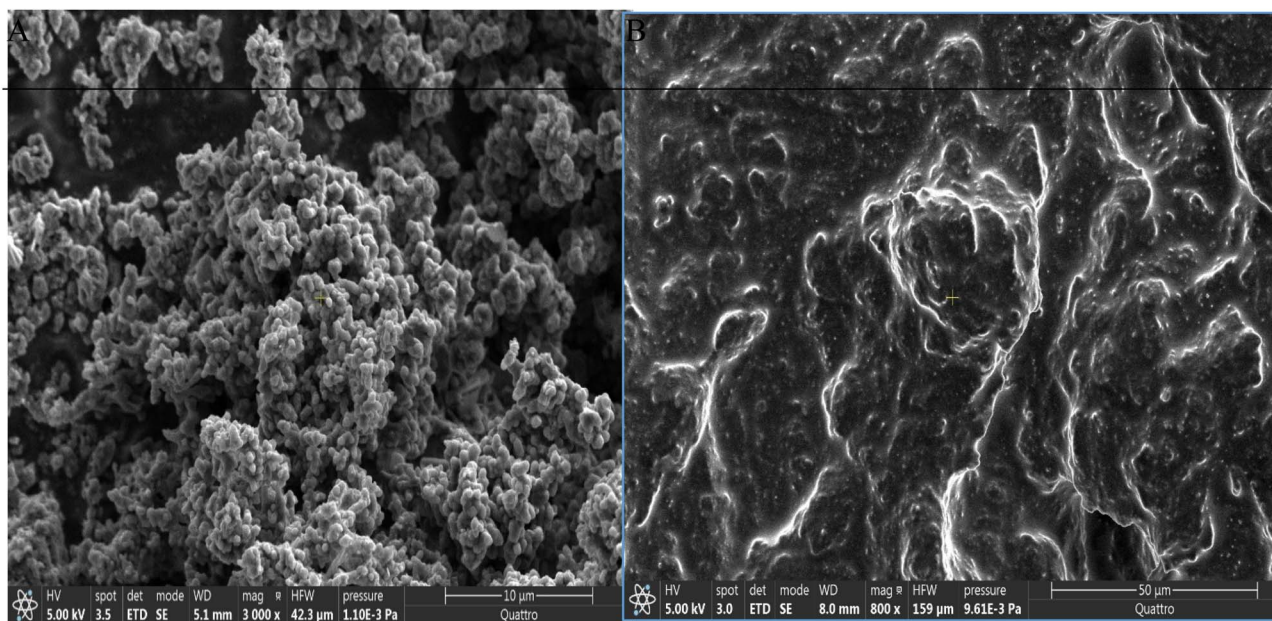

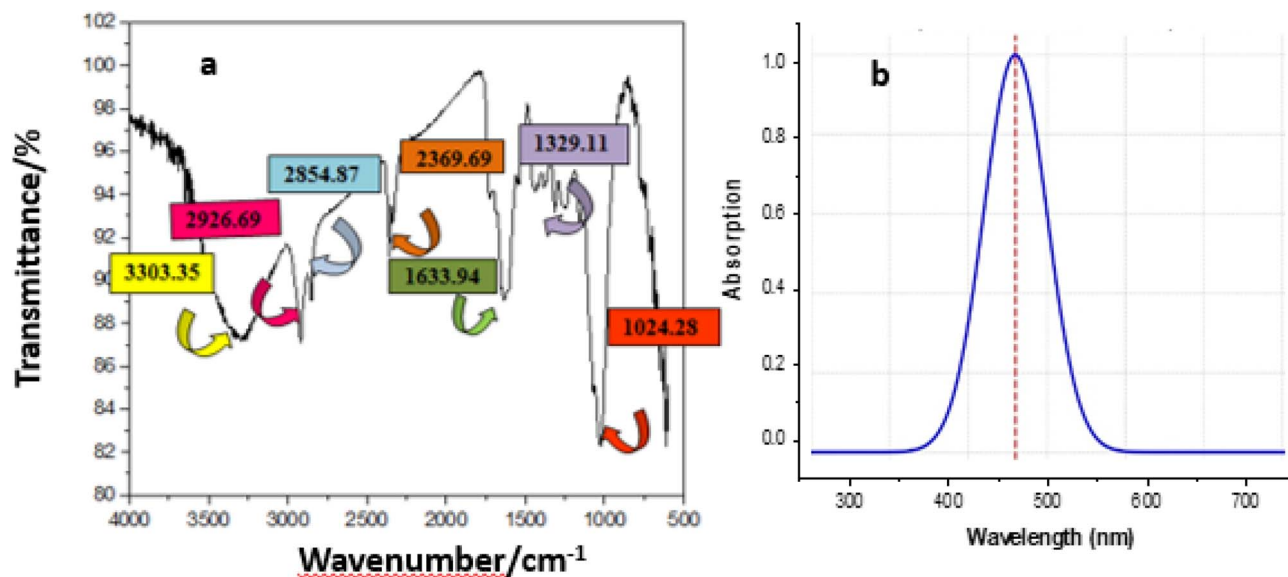Fig. 1 FEG-SEM images of: (A) polyaniline (PANI), (B) carbon paste electrode (CPE).

Fig. 3 (a) FT-IR spectra of olive leaves extract spectrum, (b) UV-Vis absorbance spectrum of green-synthesized AgNPs. (The curve shown is representative of three independent nanoparticle synthesis batches).

The band observed at 1024 cm^{-1} is indicative of C–O stretching vibrations from alcohols, ethers, or carboxylic acids.

These identified functional groups confirm the presence of biomolecules such as polyphenols, flavonoids, and amino compounds, which are known to act as natural reducing and stabilizing agents in the green synthesis of silver nanoparticles.

The UV-Vis absorption spectrum shown in Fig. 3b reveals a strong and narrow surface plasmon resonance (SPR) band centered around approximately 435 nm, which is characteristic of the formation of colloidal silver nanoparticles. This plasmonic peak arises from the collective oscillation of conduction electrons at the surface of silver nanoparticles when excited by light, and it is highly sensitive to particle size, shape, distribution, and the surrounding medium.

The appearance of a single, sharp peak indicates that the synthesized AgNPs are spherical, well-dispersed, and relatively uniform in size, with little to no aggregation. According to recent studies, silver nanoparticles typically exhibit SPR peaks in the range of 400–450 nm when they are spherical and smaller than 50 nm.[29] The observed maximum at ∼435 nm supports the formation of small-sized AgNPs with good stability and minimal agglomeration.

The SPR absorption peak at 435 nm and the brown color of the colloidal dispersion are consistent with the presence of moderately large or slightly aggregated silver nanoparticles, as previously reported in similar green synthesis protocols[30,31]

Moreover, the absence of any additional peaks at longer wavelengths confirms the lack of significant particle aggregation or the presence of anisotropic shapes (*e.g.*, rods or triangular plates), which would otherwise shift the SPR band to higher wavelengths.[32]

This result confirms the successful green synthesis of AgNPs using a biological or plant-mediated reducing agent, which is known to produce nanoparticles with controlled morphology and good stability under mild conditions.[33]

3.2. Optimization of experimental conditions

The influence of deposition potential and deposition time on the electrochemical response of Cd^{2+} and Pb^{2+} ions (100 μg L^{-1} each) was investigated using square wave voltammetry in 0.1 M acetate buffer (pH 4.5). These parameters are critical for optimizing the preconcentration step, which directly affects the sensitivity and selectivity of the sensor. The peak currents of both Cd^{2+} and Pb^{2+} increased as the deposition potential became more negative, reaching a maximum at −1.0 V. Beyond this value, the current began to decrease slightly, likely due to the onset of hydrogen evolution, which interferes with metal ion deposition. Therefore, −1.0 V was chosen as the optimal deposition potential, balancing efficient reduction of metal ions with minimal interference. An increase in deposition time led to a proportional increase in the stripping peak currents for both ions, reflecting greater accumulation of metal ions on the electrode surface. However, the current tended to plateau beyond 120 seconds, indicating saturation of the active sites on the modified sensitivity and reasonable analysis time.

On the other hand, the electrolyte solution pH has a significant role in electrochemical determination of metal ions. In Fig. 4c, Cd^{2+} and Pb^{2+} current response. It can be observed that peaks current gradually increase reaching an optimal value for pH = 4.5. For electrolytes with pH greater than 4.5.

These results confirm that the AgNPs-PANI-modified carbon paste electrode provides effective preconcentration and detection of Cd^{2+} and Pb^{2+} under optimized conditions, demonstrating its suitability for trace-level monitoring in aqueous media.
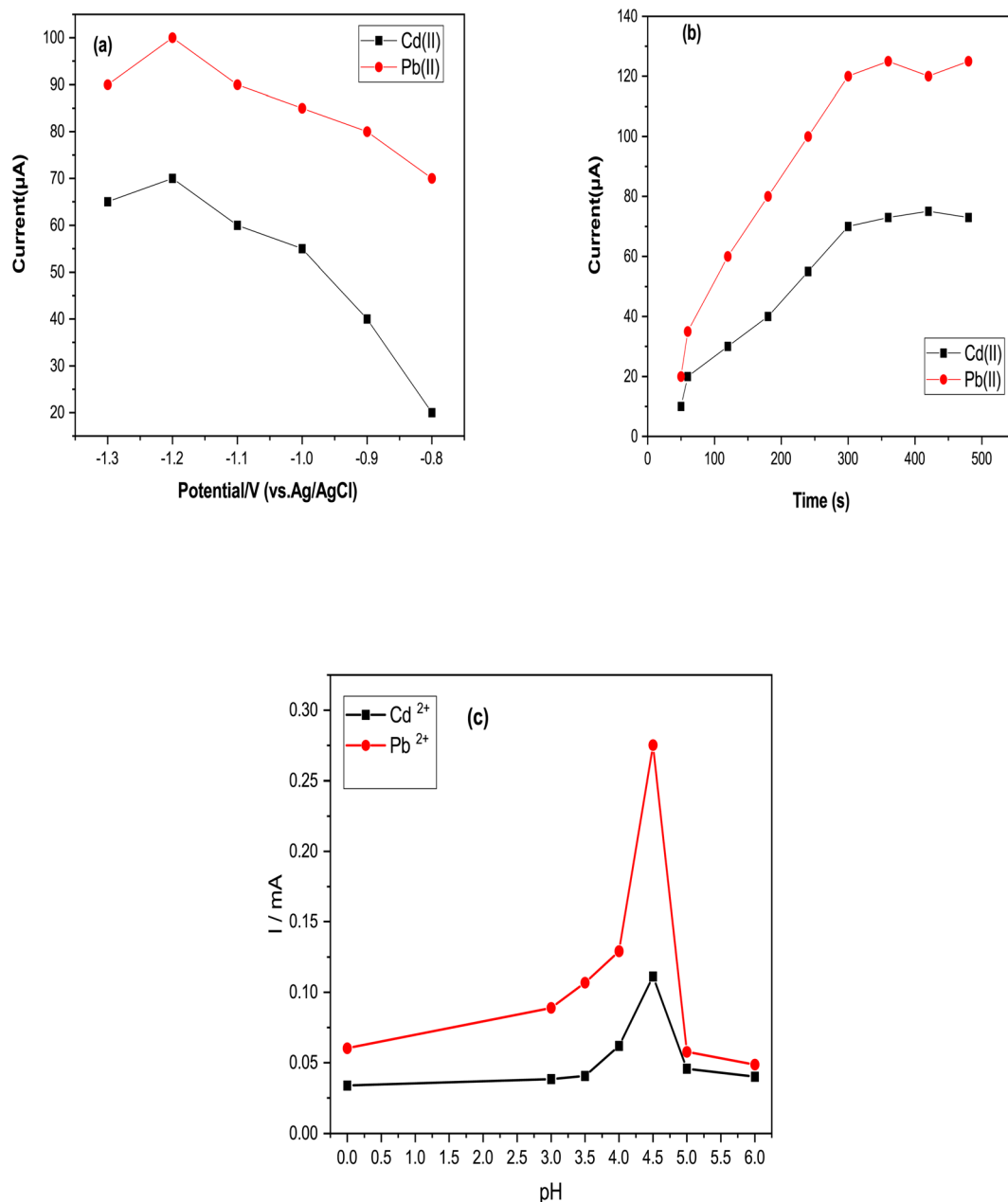
Fig. 4 Effect of (a) deposition potential, (b) deposition time on the anodic stripping peak current of Cd^{2+} and Pb^{2+} of 100.0 µg L^{-1} to evaluate AgNPs-PANI-CPE sensor performance in 0.1 M acetate buffer (pH 4.5) and (c) anodic peak currents in acetate buffer as a function of pH (each point represents the mean ± standard deviation (SD) of three independent measurements).

3.3. Electrochemical characterization

The CV curves were recorded at various scan rates ranging from 10 to 120 mV s^{-1}. As observed, the peak current (I_p) increases progressively with the increase in the scan rate (v). The anodic and cathodic peaks become more pronounced and shift slightly, which is characteristic of a quasi-reversible electrochemical process.

The effect of the potential scan on the electrochemical behavior of the elaborated electrode was performed using potassium ferrocyanide–ferricyanide probe solution containing 5 mM $[Fe(CN)_6]^{3-/4-}$ and 0.1 M KCl (Fig. 5).

As illustrated in Fig. 6A, both the anodic and cathodic peak currents increased progressively with rising scan rates.

Furthermore, a linear correlation was observed between the peak current and the square root of the scan rate, confirming a diffusion-controlled electrochemical process. The corresponding linear regression equations are as follows:

$$I_{pa}/\mu A = 0.00404v^{1/2}\ (mV\ s^{-1}) + 0.0003,\ R^2 = 0.9902 \quad (3)$$

$$I_{pc}/\mu A = -0.0045v^{1/2}\ (mV\ s^{-1}) - 0.0003,\ R^2 = 0.995 \quad (4)$$

This linearity is a hallmark of a diffusion-controlled redox process, which is further corroborated by the plot of log(i) *versus*
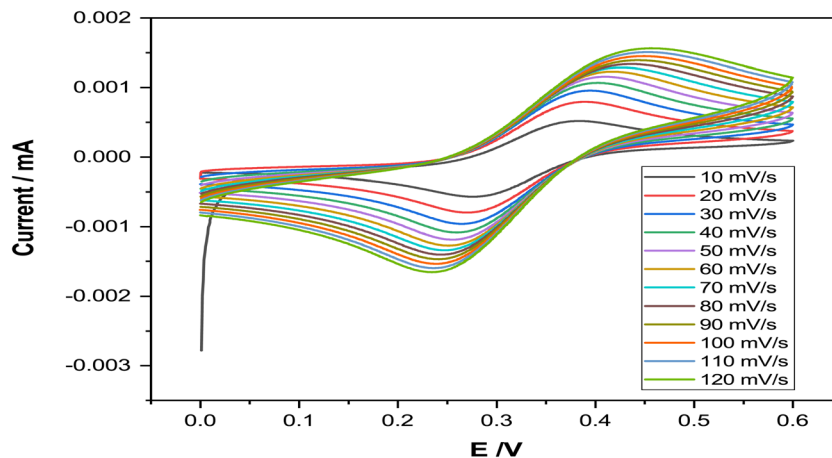
Fig. 5 Cyclic voltammograms of AgNPs-PANI-CPE electrode at scan rates from 10 to 120 mV s^{-1} in [Fe(CN)$_6$]$^{3-/4-}$ solution. (Representative voltammograms from triplicate experiments).
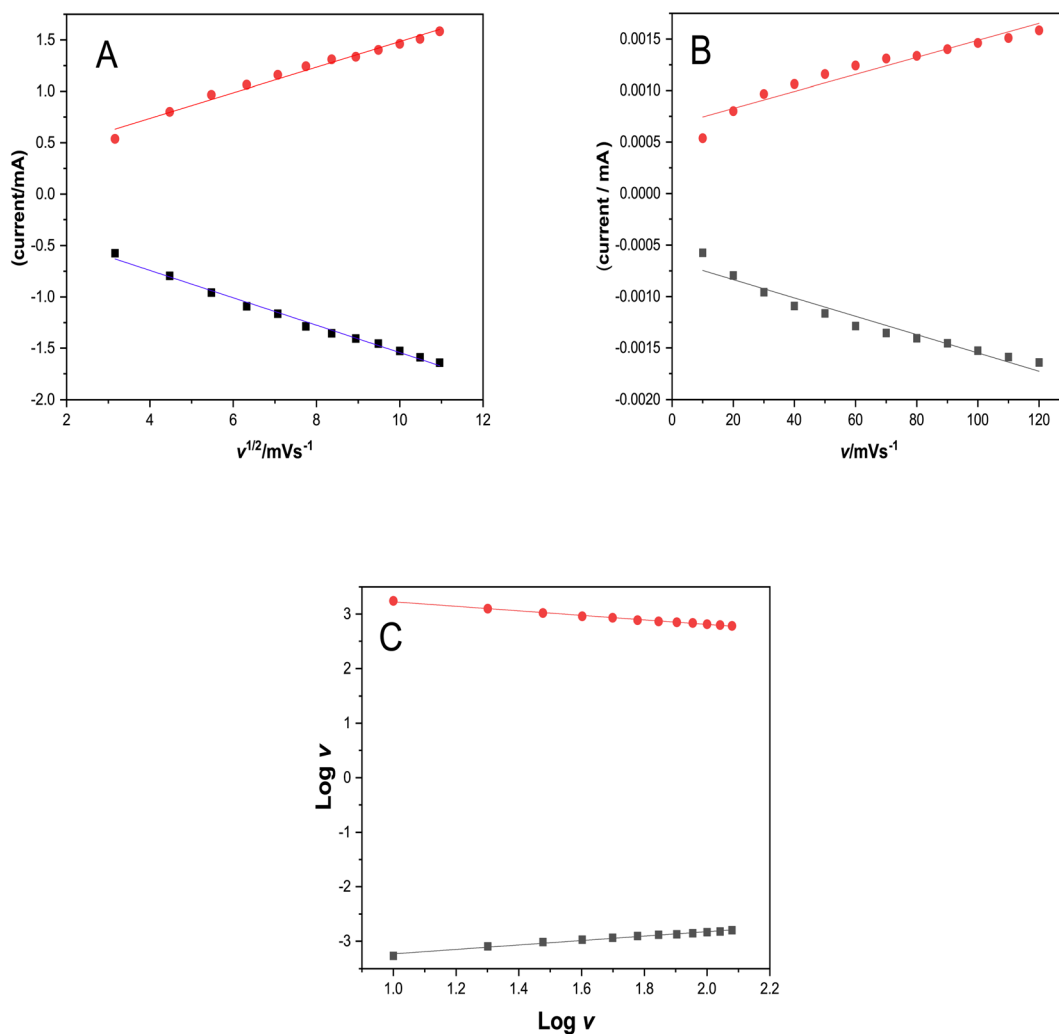

Fig. 6 (A) Plot of anodic and cathodic peak currents *vs.* square root of scan rates; (B) peak currents *vs.* scan rates and (C) log of peak currents *vs.* logarithm of scan rates for AgNPs-PANI-CPE (all plots are based on average values from three independent measurements; error bars represent ± SD).

Table 1 Electrochemical parameters of CV curves after each modification

Electrode	CPE	PANI-CPE	AgNPs-PANI-CPE
A (cm^2)	0.25	0.28	0.50
ΔE_p (mV)	0.34	0.19	0.15
I_{pc}/I_{pa}	1.09	1.22	1.12

$\log(\nu)$ (Fig. 6C), showing a linear relationship indicative of diffusion-governed kinetics.

To quantitatively assess the electroactive surface area of the bare and modified carbon paste electrodes (CPE), the slopes obtained from eqn (3) and (4) were utilized in the Randles–Ševčík equation:[34,35]

$$I_{pa} = 2.69 \times 10^5 n^{(3/2)} D^{(1/2)} A C \nu^{(1/2)} \quad (5)$$

where n, ν, C, A, and D represent the number of electrons exchanged ($n = 1$), the scan rate, the bulk concentration, the electroactive surface area, and the diffusion coefficient of 5 mM of $[Fe(CN)_6]^{3-/4-}$ in 0.1 M KCl, respectively. The calculated values of the real electroactive surface areas are summarized in Table 1.

As shown in Table 1, the electroactive surface area increases progressively with each step of electrode modification, indicating a successful enhancement of the electrode surface and improved electron transfer properties.

The cyclic voltammograms shown in Fig. 7a reveal significant differences between the bare CPE and the progressively modified electrodes, particularly in terms of peak current intensities, the potential separation between anodic and cathodic peaks (ΔE_p), and the anodic-to-cathodic peak current

ratio (I_{pa}/I_{pc}). These electrochemical parameters are summarized in Table 1. The observed variations not only confirm the successful modification of the electrode surface, but also indicate a shift toward a more reversible redox system upon incorporation of PANI and AgNPs.

Electrochemical impedance spectroscopy (EIS) measurements were conducted to investigate the electron transfer behavior at the surface of the carbon paste electrode (CPE) before and after modification. The Nyquist plots presented in Fig. 7a display semicircles in the high-frequency region, characteristic of charge transfer processes at the electrode/electrolyte interface. For the unmodified CPE, the observed semicircle corresponds to a charge transfer resistance (R_{ct}). Upon modification with polyaniline (PANI), the semicircle diameter decreased significantly, indicating a reduction (green curve). This decrease reflects enhanced electron transfer kinetics attributed to the conductive nature of the PANI layer.

Further deposition of (AgNPs) onto the PANI-modified CPE resulted in a further decrease, suggesting an improved interfacial charge transfer process. This enhancement is likely due to the synergistic effect between PANI and AgNPs, which modified the electrode surface properties and facilitates electron transport.

Overall, these results demonstrate that the AgNPs-PANI-CPE exhibits superior charge transfer performance compared to the bare CPE, confirming the beneficial role of surface modification in enhancing electrochemical activity.

3.4. Simultaneous detection of Cd^{2+} and Pb^{2+}

The square wave voltammetry (SWV) responses in Fig. 8 recorded for the simultaneous detection of Cd^{2+} and Pb^{2+} using three
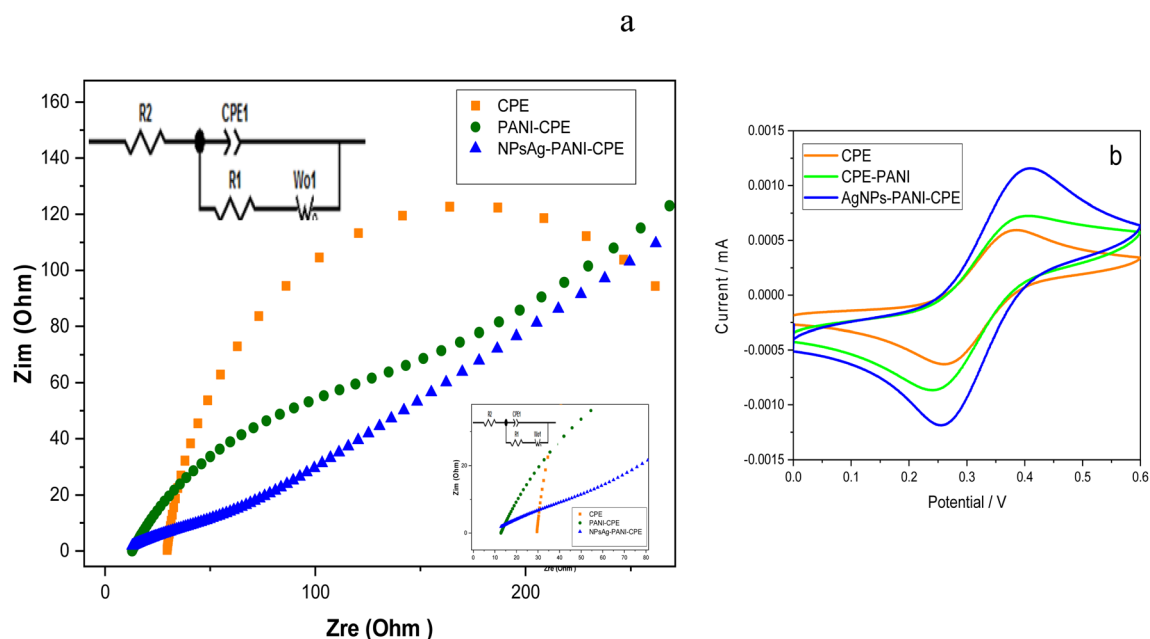
Fig. 7 (a) Nyquist diagram of CPE, PANI-CPE, and AgNPs-PANI-CPE [inset: the equivalent circuit], (b) CV curves of CPE, PANI-CPE, AgNPs-PANI-CPE in 5 mM $[Fe(CN)_6]^{3-/4-}$ solution containing 0.1 M KCl at scan rate of 50 mV s^{-1}.
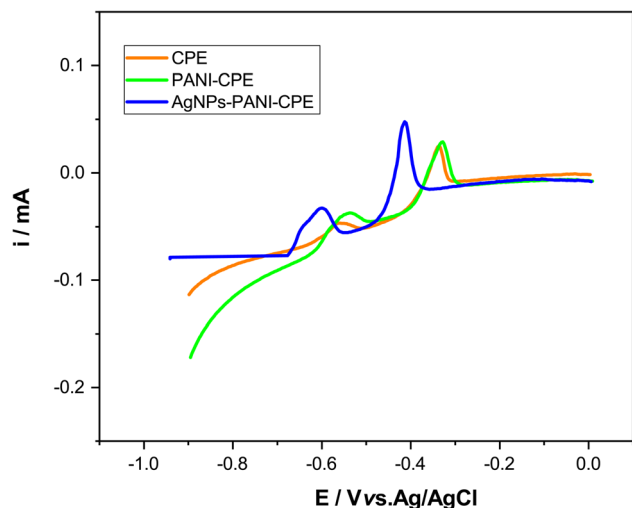
Fig. 8 Comparison of SWV on these three different electrodes for simultaneous detection of 4.8 µg L^{-1} Cd^{2+} and Pb^{2+}.

the most distinct separation between the Cd^{2+} and Pb^{2+} peaks. This enhancement is attributed to the synergistic effect between PANI and AgNPs, which increases the electroactive surface area and promotes more efficient preconcentration and redox reaction of the target ions.

These results confirm that the PANI/AgNPs-modified CPE offers superior performance for the simultaneous detection of Cd^{2+} and Pb^{2+} compared to the bare or singly modified electrodes.

Fig. 9 presents the simultaneous detection of a mixture of Cd^{2+} and Pb^{2+} in the concentration range of 0.1 to 6 µg L^{-1}, carried out under optimized conditions using the AgNPs-PANI-CPE electrode in. 0.1 M acetate buffer (pH 4.5) The square wave voltammetry responses exhibit a progressive increase in peak currents with increasing concentrations of the two metal ions. A slight positive shift in peak potentials was observed as concentrations increased, which due to changes in mass transport and interfacial kinetics. Nevertheless, the individual peaks corresponding to Cd^{2+} and Pb^{2+} remained well-defined and clearly separated. Remarkably, the sensitivity and linearity of the sensor towards each metal ion were maintained, and no significant shift in peak positions was observed when compared to their individual detections. These results indicate the absence of mutual interference among the ions during simultaneous determination.

Peaks current increase with metal ions concentration increase, giving a linear relationship between peak current amplitude and concentration. The limit of detection (LOD) (S/N = 3) for Cd^{2+} and Pb^{2+} were calculated to be 0.09 µg L^{-1} and 0.05 µg L^{-1}, respectively.

To evaluate the simultaneous detection of the metal ions (Cd^{2+} and Pb^{2+}) in 0.1 M acetate buffer (pH 4.5) using the AgNPs-

different working electrodes demonstrate clear differences in peak intensity and definition.

The unmodified carbon paste electrode (CPE) exhibits weak and poorly defined peaks for both metal ions, indicating low sensitivity and limited electrocatalytic activity.

Upon modification with polyaniline (PANI), a noticeable enhancement in peak current is observed for both Cd^{2+} and Pb^{2+}, suggesting improved conductivity and electron transfer kinetics due to the conductive polymer film.

The electrode further modified with green-synthesized silver nanoparticles (AgNPs) displays the highest peak currents and
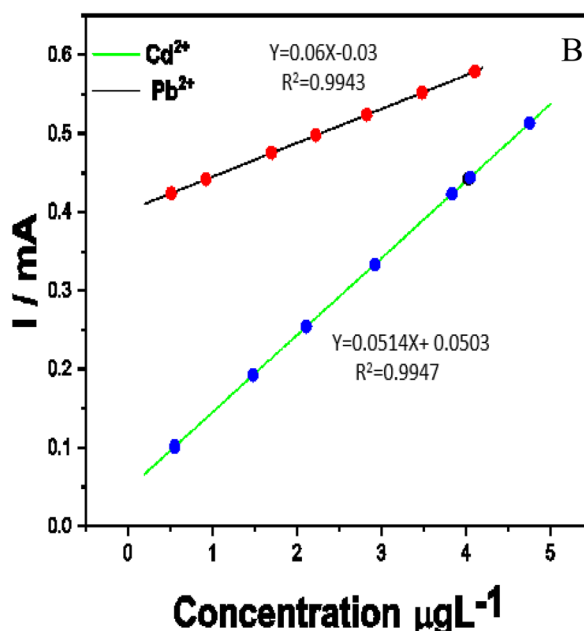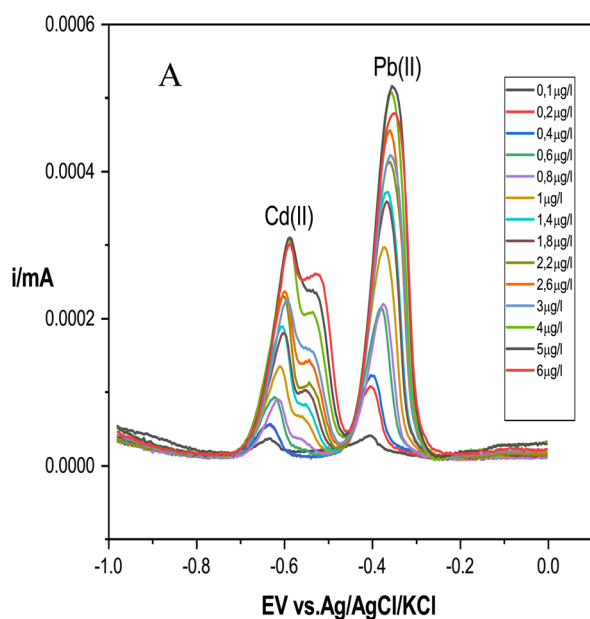

Fig. 9 A) Multi metal SWV of AgNPs-PANI-CPE in 0.1 M acetate buffer (pH 4.5) for the simultaneous detection of Cd^{2+} and Pb^{2+}. (B) The corresponding the calibration curves.
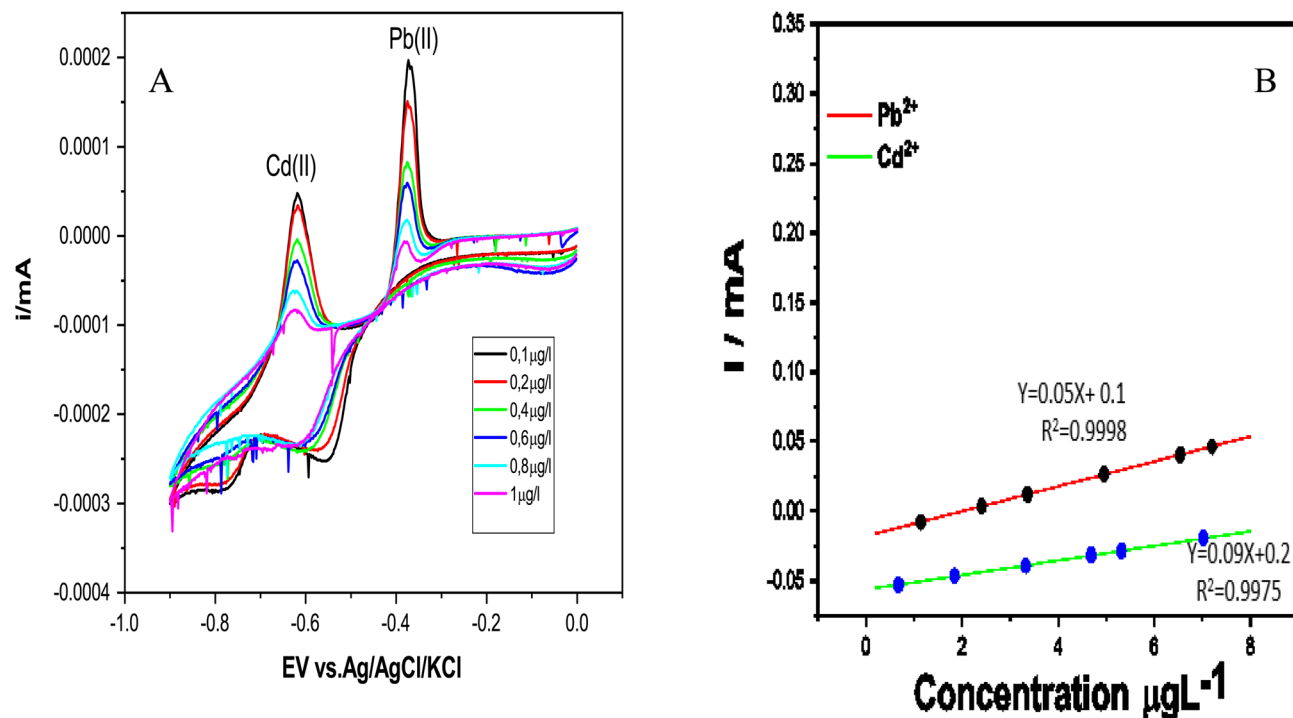
Fig. 10 A) CV Curves for simultaneous analysis of AgNPs-PANI-CPE in 0.1 M acetate buffer (pH 4.5) containing [0.1–1] µg L^{-1} of Cd^{2+} and Pb^{2+} at scan rate of 50 mV s^{-1}. (B) The corresponding: the calibration curve.

PANI-CPE electrode, cyclic voltammetry was performed within the potential window of −0.1 to 0.7 V at a scan rate of 50 mV s^{-1} (see Fig. 10). As anticipated, similar electrochemical behavior was observed in the multi-metal system, characterized by a progressive increase in peak currents with rising metal ion concentrations. This behavior resulted in a linear correlation for Cd^{2+} and Pb^{2+}. The limits of detection (LOD) were estimated at 0.27 µg L^{-1} for Cd^{2+}, 0.15 µg L^{-1} for Pb^{2+}.

Moreover, the newly developed electrode fabrication approach demonstrated a favorable linear response range and low detection limits. A comparison of the analytical performance parameters with those reported for various electrochemical sensors in previous studies highlights the superior performance of the AgNPs-PANI-CPE sensor, as summarized in Table 2.

The results presented in this work demonstrate the successful development of an eco-friendly electrochemical sensor with competitive analytical performance compared to recent studies. For instance, the detection limits for Cd^{2+} (0.09 µg L^{-1} by SWV) and Pb^{2+} (0.05 µg L^{-1} by SWV) are lower or comparable to those reported using more complex or expensive electrode modification techniques.[36–41]

Table 2 Comparison of sensor's ion detection capabilities with other electrodes reported in the literature[a]

Modified electrode	Method	Detection limit		Linear range		Ref.
		Cd^{2+}	Pb^{2+}	Cd^{2+}	Pb^{2+}	
M-γ-Al$_2$O$_3$-CPE	DPASV	0.20 nmol L^{-1}	2.0 nmol L^{-1}	0.001–10 µmol L^{-1}	0.001–10 µmol L^{-1}	36
2H5MA-MOF	SWASV	5.77 × 10^{-2} ppm	—	0–2 ppm	—	37
UiO-66-NH$_2$-Mxene@rGO/GCE	DPASV	0.4 6 ppb	0.40 ppb	5–300 ppb	5–300 ppb	38
CPE/PANI-PDTDA	DPSV	0.29 ppb	0.17 ppb	—	—	39
BiONPs/PANI/SPCE	SWV	—	0.49 ppb	—	0.45–5.43 µM	40
Ag$_2$WO$_4$ NC	SWASV	10–260 ppb	—	—	2.022 ppb	41
AgNPs-PANI-CPE	CV SWV	0.27 µg L^{-1}	0.15 µg L^{-1}	0.1–1 µg L^{-1}	0.1–1 µg L^{-1}	This work
		0.09 µg L^{-1}	0.05 µg L^{-1}	0.1–2.6 µg L^{-1}	0.1–2.6 µg L^{-1}	

[a] Ionic liquid/CNF/Bi/CPE: ionic liquid/carbon nanofibers/bismuth/carbon past electrode; BiONPs/PANI/SPCE: bismuth oxide nanoparticles/polyaniline/screen-printed electrode; CPE/PANI-PDTDA: carbon past electrode/polyaniline-2,5-bis(4-aminophenyl)-1,3,4-thiadiazole; UiO-66-NH$_2$-Mxene@rGO/GCE: UiO-66-NH$_2$ (Zr-based MOF)/Mxene nanosheetd anchored on reduced graphene oxide/glassy carbon electrode; Ag$_2$WO$_4$ NC: silver tungstate nanocrystals; (M-γ-Al$_2$O$_3$): anosized mesoporous γ-alumina; AgNPs-PANI-CPE: silver nanoparticles-polyaniline-carbon paste electrode.

Moreover, the simultaneous detection capability with well-resolved peaks and minimal interference highlights the advantage of using a synergistic nanocomposite consisting of polyaniline and green-synthesized AgNPs. Compared to previous reports such as UiO-66-NH$_2$-Mxene@rGO/GCE[38] or

BiONPs/PANI/SPCE,[40] the proposed sensor offers a simpler fabrication process, lower cost, and greener synthesis pathway, while maintaining excellent sensitivity and selectivity.

Therefore, this work contributes to the growing field of green electroanalytical chemistry by proposing a sustainable, low-cost sensor platform for environmental monitoring of toxic metal ions in water systems. The integration of biogenic nano-materials with conducting polymers provides a scalable strategy that can be further optimized for broader environmental applications.

4.   Method validation

4.1.   Interference examination

The AgNPs-PANI-CPE sensor was evaluated for its selectivity in detecting the target metal ions (Cd^{2+} and Pb^{2+}) in 0.1 M acetate buffer (pH 4.5) the presence of various potential interfering substances. Square wave voltammetry (SWV) measurements were carried out in 0.1 M acetate buffer (pH 4.5) solution containing 50 μg L^{-1} of each target ion, while progressively adding common interfering ions such as Ag^+, Al^{3+}, Cr^{3+}, Fe^{3+}, Fe^{2+}, Mg^{2+}, Ni^{2+}, and Zn^{2+}.

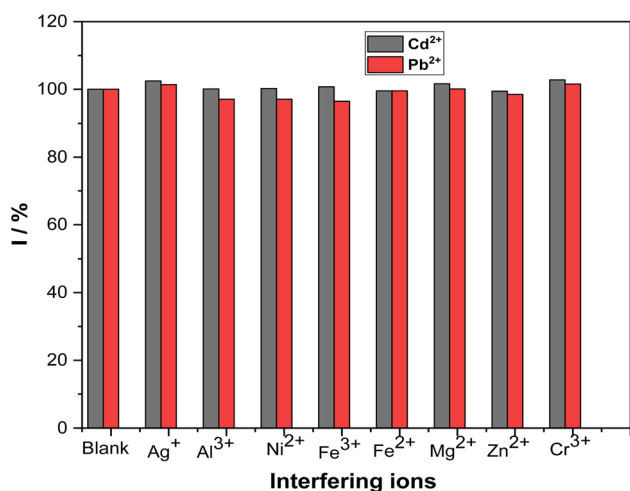As shown in Fig. 11, despite the interfering ions being present at concentrations ten times higher than those of the

Fig. 11 Responses of AgNPs-PANI-CPE towards Cd^{2+} and Pb^{2+} in the presence of different interfering substances.

Table 3 Detection of Cd^{2+} and Pb^{2+} in real waters using AgNPs-PANI-CPE electrode using by SWV method

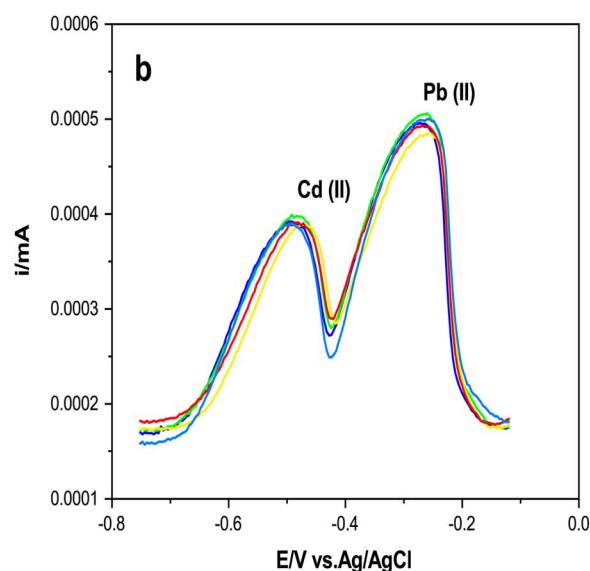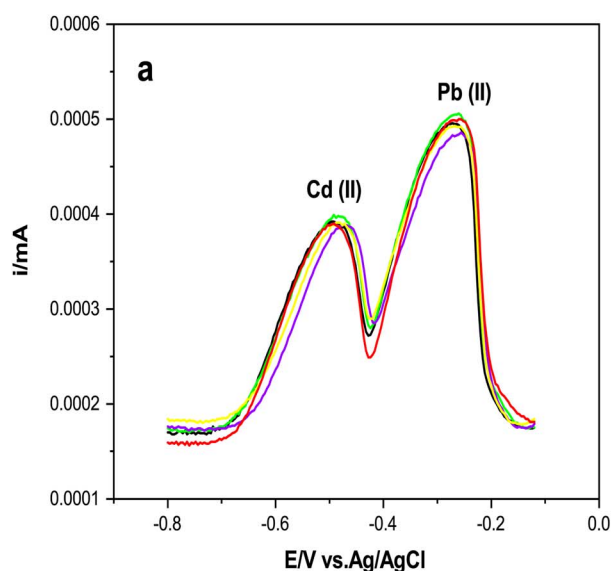| Sample	Cd^{2+} spiked (μg L^{-1})	Cd^{2+} found (μg L^{-1})	Recovery (%) Cd^{2+}	Pb^{2+} spiked (μg L^{-1})	Pb^{2+} found (μg L^{-1})	Recovery (%) Pb^{2+}
Sea water	0.0	0.0	—	0.0	0.0	—
	0.5	0.6	112	0.5	0.7	114
	1.0	1.3	113	1.0	1.0	100
	1.5	1.5	100	1.5	1.7	113.33
	2.5	2.7	108	2.5	2.3	92

Fig. 12 SWV recorded in Cd^{2+} and Pb^{2+} in 0.1 M acetate buffer (pH 4.5) on AgNPs-PANI-CPE for (a) repeatability experiments and (b): sensor stability over a 14 days.

analytes, no significant changes in the response signals were observed. These findings confirm the excellent anti-interference capability of the AgNPs-PANI-CPE sensor for the simultaneous detection of heavy metal ions.[42]

4.2. Real sample analysis

The practical applicability of the AgNPs-PANI-CPE sensor was further assessed through the simultaneous detection of Cd^{2+} and Pb^{2+} in real water samples (seawater), the recovery values, summarized in Table 3, ranged from 92% to 114%, demonstrating the reliability and accuracy of the sensor in complex matrices. The favorable recovery rates and detection accuracy illustrate the strong potential of the AgNPs-PANI-CPE sensor for environmental monitoring applications.[43]

4.3. Repeatability, reproducibility, and stability

For repeatability, three successive measurements of 1.0 μg L^{-1} Cd^{2+} and Pb^{2+} were performed under identical conditions using the same electrode. The relative standard deviation (RSD) values were found to be below 3.0%, indicating good short-term precision (Fig. 12a).

To assess reproducibility, three independently prepared AgNPs-PANI-CPE electrodes were tested under the same conditions. The RSD values remained below 4.2%, confirming that the fabrication process is consistent and reproducible.

The stability of the modified electrode was tested by storing it at room temperature and measuring its response every two days over a period of 14 days. The sensor retained more than 92% of its initial signal, demonstrating excellent operational stability and suitability for routine analysis (Fig. 12b).

5. Conclusion

In this study, a green-synthesized silver nanoparticle and polyaniline-modified carbon paste electrode (AgNPs-PANI-CPE) was successfully developed and applied for the simultaneous electrochemical detection of Cd(II) and Pb(II) ions. The surface characterization confirmed the effective integration of uniformly dispersed AgNPs onto the conductive PANI matrix, enhancing the electrode's active surface area and electron transfer capabilities. Electrochemical investigations using cyclic voltammetry (CV) and square wave voltammetry (SWV) demonstrated the high sensitivity, selectivity, and reproducibility of the modified electrode for detecting trace levels of the target heavy metals. The method showed low detection limits, good linearity, and strong potential for practical application in environmental monitoring, particularly in marine environments. This eco-friendly approach not only provides an efficient sensing platform but also aligns with sustainable development goals by utilizing green synthesis methods and promoting low-cost sensor fabrication.

Future work will focus on improving the stability and reusability of the sensor, extending the detection to other heavy metals (e.g., Hg^{2+}, As^{3+}), and applying the electrode in real field scenarios with varied water matrices. Moreover, the use of other

plant-based extracts or biopolymers may be explored to develop new green nanocomposites for electrochemical sensing.

Conflicts of interest

The authors declare that there are no conflicts of interest.

Data availability

All data supporting the findings of this study are included within the manuscript. No additional datasets or supporting files are available.

References

1 L. Järup, Fr. Méd. Bull., 2003, 68, 167–182.
2 P. B. Tchounwou, C. G. Yedjou, A. K. Patlolla and D. J. Sutton, Exper. Suppl., 2012, 101, 133–164.
3 Organisation mondiale de la santé (OMS), Directives pour la qualité de l'eau potable, 2022.
4 A. Isa, M. Gharibi, A. Cetinkaya and S. A. Ozkan, Microchem. J., 2025, 212, 113210.
5 N. Esfandiari and M. Aliofkhazraei, Talanta, 2024, 277, 126365.
6 M. Babankumar and S. Bansod, Microchem. J., 2025, 212, 113188.
7 I. Tomac, V. Adam and J. Labuda, Food Chem., 2024, 460, 140548.
8 D. Slimane Ben Ali, F. Krid, M. Nacef, M. L. Chelaghmia, E. Boussaha, H. Tabet, R. Selaimia, A. Atamnia and A. M. Affoune, RSC Adv., 2023, 13, 18734–18747.
9 M. Yang, H. Zhang, L. Wang and C. He, Microchim. Acta, 2015, 182, 2091–2104.
10 S. Cohen, I. Chajanovsky and R. Y. Suckeveriene, Polymers, 2025, 17(10), 1320.
11 M. Tayyab, A. Rahim, M. Tariq, Z. H. Khan, S. Sabahat, J. Iqbal, D. ouad, A. Qadeer, F. S. Ataya and L. Sherin, J. Water Process Eng., 2025, 75, 107927.
12 S. Tajik, H. Beitollahi, F. G. Nejad, I. S. Shoaie, M. A. Khalilzadeh, M. S. Asl, Q. V. Le, K. hang, H. W. Jang and M. Shokouhimehr, RSC Adv., 2020, 10, 37834–37856.
13 N. Awoke, G. Beyene, F. Tolassa, M. Asfew, P. M. Ejikeme, A. C. Nwanya and F. I. Ezema, Appl. Phys. A, 2025, 131, 367.
14 S. Ahmed, M. Ahmad, B. L. Swami and S. Ikram, J. Radiat. Res. Appl. Sci., 2016, 9, 1–7.
15 S. Shahzadi, S. Fatima, Q. ul ain, Z. Shafiq and M. R. S. A. Janjua, RSC Adv., 2025, 15, 3858–3903.
16 M. Ohiduzzaman, M. N. I. Khan, K. A. Khan, B. Paul, M. Nazmul, H. Zilani and M. N. Hasan, Heliyon, 2024, 10(11), e32419.
17 A. Khan, M. Anas, F. Bibi, M. Ali, A. T. Khalil, K. S. Munawar, H. E. A. Mohamed, K. Hkiri, M. Maaza and Z. K. Shinwari, Appl. Biochem. Biotechnol., 2025, 197, 3630–3667.
18 S. Iravani, Green Chem., 2011, 13, 2638–2650.
19 K. S. Prasad, A. Pathan, A. S. Patel, P. Dalwadi, N. Gajera and R. P. Patel, Int. J. Nanomed., 2011, 6, 219–225.

20 A. A. Enafi, K. A. Al-Ghamdi, M. A. Al-Fandi and A. M. A. Almajid, *Electrochim. Acta*, 2014, **125**, 232–240.

21 Z. Wang, Y. Zheng, X. Wang and X. Liu, *J. Electroanal. Chem.*, 2019, **837**, 88–95.

22 K. Sahu, R. Kurrey and A. Kumar Pillai, *RSC Adv.*, 2024, **14**, 23240–23256.

23 M. M. Hossain, A. Hamza, S. A. Polash, M. H. Tushar, M. Takikawa, A. Bhowmik Piash, C. Dekiwadia, T. Saha, S. Takeoka and S. R. Sarker, *RSC Pharm.*, 2024, **1**, 245–258.

24 M. M. Y. Zaghloul, S. Ebrahim, M. Anas, M. Soliman and J. El Nady, *Electrochim. Acta*, 2024, **475**, 143631.

25 A. Thomas, *BioPharm*, 2015, **28**(4), 48–51.

26 M. Ayad, G. El-Hefnawy and S. Zaghlol, *Chem. Eng. J.*, 2013, **217**, 460–465.

27 P. Das, A. B. Deoghare and S. R. Maity, *J. Ceram. Int.*, 2022, **48**, 11031–11042.

28 P. Singh, K. RB Singh, J. Singh, S. N. Das and R. P. Singh, *RSC Adv.*, 2021, **11**, 18050–18060.

29 S. Ahmed, M. Ahmad, B. L. Swami and S. Ikram, *J. Adv. Res.*, 2016, **7**, 17–28.

30 P. Gupta, S. Singh, N. Rai, A. Verma, H. Tiwari, S. C. Kamble, H. K. Gautam and V. Gautam, *RSC Adv.*, 2024, **14**, 4074–4088.

31 S. Iravani, H. Korbekandi, S. V. Mirmohammadi and B. Zolfaghari, *Res. Pharm. Sci.*, 2014, **9**(6), 385–406.

32 N. Khatoon, J. A. Mazumder and M. Sardar, *Arab. J. Chem.*, 2020, **13**, 824–838.

33 P. Singh, S. Pandit, V. R. S. S. Mokkapati, A. Garg, V. Ravikumar and I. Mijakovic, *Int. J. Mol. Sci.*, 2018, **19**, 1979.

34 M. Gogoi, R. J Mascarenhas, A. K. Satpati, O. J. D'Souza and A. Dey, *Mater. Sci. Eng. C*, 2017, **73**, 552–561.

35 M. L. Chelaghmia, M. Nacef, A. M. Affoune, M. Pontié and T. Derabla, *Electroanalysis*, 2018, **30**, 1117–1124.

36 X. Zheng, S. Chen, J. Chen, Y. Guo, J. Peng, X. Zhou, R. Lv, J. Lin and R. Lin, *RSC Adv.*, 2018, **8**, 7883–7891.

37 A. A. A. Sari, S. O. Alzahrani, I. S. S. Alatawi, M. M. Aljohani, R. Shah, F. A. Saad, M. A. Khalil and N. M. El-Metwaly, *Spectrochim Acta A Mol Biomol Spectrosc.*, 2025, **324**, 124989.

38 J. Dong, X. Li, L. Wen, Y. Ma, J. Xu, H. Luo, J. Hou, C. Hou and D. Huo, *Food Chem.*, 2024, **437**, 137835.

39 B. Habibi, S. Pashazadeh, A. Pashazadeh and L. A. Saghatforous, *RSC Adv.*, 2023, **13**, 29931–29943.

40 E. COKpara, S. Che Nde, O. E. Fayemi and E. Ebenso, *Nanomater.*, 2021, **14**(11), 1294.

41 F. Mashkoor, M. Shoeb, S. Zhu, J. Ahmed and C. Jeong, *Mater. Chem. Phys.*, 2025, **335**, 130519.

42 Y. hou, R. Zhou, C. Zhang, Y. Yi, Y. He and G. Zhu, *J. Electrochem. Soc.*, 2024, **171**, 016504.

43 A. Qureshi, A. Shah, F. Jan Iftikhar, A. Haleem and M. A. Zia, *RSC Adv.*, 2024, **14**, 36633–36655.